Journal of Hazardous Materials 166 (2009) 394–406

Contents lists available at ScienceDirect

Journal of Hazardous Materials

journal homepage: www.elsevier.com/locate/jhazmat

Large eddy simulation of fire-induced buoyancy driven plume dispersion in an urban street canyon under perpendicular wind flow

L.H. Hu*, R. Huo, D. Yang

State Key Laboratory of Fire Science, University of Science and Technology of China, Hefei, Anhui 230026, China

ARTICLE INFO

Article history:
Received 21 April 2008
Received in revised form
12 November 2008
Accepted 13 November 2008
Available online 3 December 2008

Keywords:
Street canyon
Buoyancy driven plume
Dispersion
FDS
Critical re-entrainment wind velocity

ABSTRACT

The dispersion of fire-induced buoyancy driven plume in and above an idealized street canyon of 18 m (width) × 18 m (height) × 40 m (length) with a wind flow perpendicular to its axis was investigated by Fire Dynamics Simulator (FDS), Large Eddy Simulation (LES). Former studies, such as that by Oka [T.R. Oke, Street design and urban canopy layer climate, Energy Build. 11 (1988) 103–113], Gayev and Savory [Y.A. Gayev, E. Savory, Influence of street obstructions on flow processes within street canyons. J. Wind Eng. Ind. Aerodyn. 82 (1999) 89–103], Xie et al. [S. Xie, Y. Zhang, L. Qi, X. Tang, Spatial distribution of traffic-related pollutant concentrations in street canyons. Atmos. Environ. 37 (2003) 3213–3224], Baker et al. [J. Baker, H. L. Walker, X. M. Cai, A study of the dispersion and transport of reactive pollutants in and above street canyons—a large eddy simulation, Atmos. Environ. 38 (2004) 6883–6892] and Baik et al. [J.-J. Baik, Y.-S. Kang, J.-J. Kim, Modeling reactive pollutant dispersion in an urban street canyon, Atmos. Environ. 41 (2007) 934–949], focus on the flow pattern and pollutant dispersion in the street canyon with no buoyancy effect. Results showed that with the increase of the wind flow velocity, the dispersion pattern of a buoyant plume fell into four regimes. When the wind flow velocity increased up to a certain critical level, the buoyancy driven upward rising plume was re-entrained back into the street canyon. This is a dangerous situation as the harmful fire smoke will accumulate to pollute the environment and thus threaten the safety of the people in the street canyon. This critical re-entrainment wind velocity, as an important parameter to be concerned, was further revealed to increase asymptotically with the heat/buoyancy release rate of the fire.

1. Introduction

The wind flow field and pollutant transportation within urban areas have attracted great attention due to increasing urban pollutants and their adverse impacts on human health. A street canyon, as an idealized urban element, refers to a relatively narrow street with buildings lining up continuously along both sides. In China, numerous such street canyons, known as “Commercial streets”, have even been constructed in every big city. Tall buildings or shopping malls are constructed along the two sides of the “Commercial streets”. In weekends or festival days, there are crowds of peoples in these “Commercial streets”. It is a serious concern of the government for the fire safety of such “Commercial street” canyons.

Numerous studies, such as by Oka [1], Gayev and Savory [2]; Xie et al. [3], Baker et al. [4], Park et al. [5], Baik et al. [6] and Li et al. [7] have been conducted to reveal the flow pattern, vehicular emitted pollutant transportation, dilution, and removal mechanisms in street canyons. The flow pattern inside street canyons with a wind flow perpendicular to its axis as shown in Fig. 1, which was a typical scenario being concerned mostly by researchers, is revealed by Oke [1] to fall into three regimes: skimming flow, wake interference flow and isolated roughness flow, depending on the geometry of the street canyon, especially the aspect ratio (W/H), where W is the street width and H is the building height. When the street canyon is narrow, for example, the aspect ratio of 1, a recirculation flow forms inside the street canyon. The pollutant emitted at the base of street canyon is not easy to be ventilated out under this condition. It will be re-entrained back into the street canyon by the recirculation vortex formed in the street canyon and accumulates to high level.

Field measurement [3], laboratory-scale physical modelling (wind tunnel or water channel experiments) and CFD simulation [2,4,6,8–11] have been performed to study the pollutant transportation, both non-reactive and reactive, inside the street canyons. For example, Xie et al. [3] have measured the wind fields and the spatial distribution of traffic-related pollutants, including CO, NO, NO_2 and O_3, within the street canyons in Guangzhou, China. Wind tunnel studies [2,8,9] have also been performed to investigate the wind field patterns and pollutant distribution inside the street canyons. With the rapid development of computer technology, CFD

* Corresponding author. Tel.: +86 551 3606446; fax: +86 551 3601669.
E-mail address: hlh@ustc.edu.cn (L.H. Hu).

0304-3894/$ – see front matter © 2008 Elsevier B.V. All rights reserved.
doi:10.1016/j.jhazmat.2008.11.105

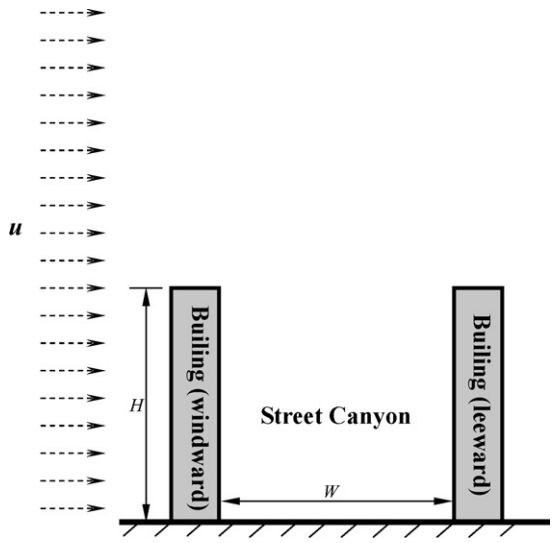

Fig. 1. Schematic of street canyon with perpendicular wind flow.

modelling is now also widely applied to study the turbulent flow and pollutant dispersion in the street canyons. Pollutant reaction was even considered associated with the wind flow dynamics simulation in recent years. Simple photochemistry of $NO–NO_2–O_3$ was introduced by Baker et al. [4] into a large eddy simulation model to examine reactive pollutant dispersion in a street canyon with a street aspect ratio of one. This model was further improved by Baik et al. [6] with temperature-dependent reaction coefficients considered.

However, it should be noted that all these former studies consider the non-buoyancy flow only. When there is a buoyancy source, for example, a fire accident occurs in the street canyon, such as burning a vehicular, harmful, even deadly, smoke plume will be generated by the fire and driven to rise up by the buoyancy force. Fire can lead to adverse impacts to the urban air quality and inhabitants health [12]. Pollutant smoke is reported [13] to be a major threat to human safety in fire environment. It was proved [14] that the main cause of death during urban fires is poisoning by the harmful smoke. In the open quiescent air with no street canyon effects, the fire plume grows up gradually and rises upward axis-symmetrically, taking the dangerous gases released by the fire combustion away from the ground level to upper air. However, when a fire occurs in the street canyon, where a recirculation flow usually forms and exists [1], it can be anticipated that there should be a complex interaction between the original wind driven recirculation flow and the buoyancy driven fire plume inside the street canyon. The buoyancy force helps the fire plume to be ventilated out of the top of the street canyon. But the perpendicular wind flow trends to form a recirculation flow in the street canyon, counteracting the ventilation. Can the fire-released pollutant smoke still be ventilated by its own buoyancy? What the flow pattern will be like in the street canyon under this condition is an interdisciplinary topic between fire research and atmospheric environment research that should be further investigated.

In this paper, the dispersion of fire-induced buoyancy driven plume under the above condition with a wind flow perpendicular to the axis of the street canyon was studied computationally. An idealized street canyon with both width and height to be 18 m, length of 40 m, the same as that used by Baker et al. [4], was considered. Large Eddy Simulation (LES) were performed by Fire Dynamics Simulator (FDS), a Computational Fluid Dynamics (CFD) model developed by National Institute of Standards and Technology (NIST) [15,16], which was validated by full scale experiments in a real road tunnel [17,18] to be capable of simulating the interaction between the cross wind flow and the large buoyant fire plume. The dispersion of buoyancy driven plume induced by fire of different sizes in this street canyon under different levels of perpendicular wind flow was studied.

2. Numerical simulation

2.1. Methodology

With rapid development in computer science and technology, Computational Fluid Dynamics (CFD) techniques are widely used [e.g., 4,6,11] to study the wind field and pollutant transport in urban street canyons, as well as to simulate buoyancy-induced flow in fire engineering [e.g., 18–22]. Turbulence methods commonly used in CFD include Reynolds Averaging Navier-Stokes equation (RANS) method, Large Eddy Simulation (LES) and Direct Numerical Simulation (DNS) [15,20,23,24].

DNS can give a most detailed simulation on the flow, but requiring too much computing resources. DNS is not yet practical in fire engineering, as it is still not yet possible with updated hardware to simulate small turbulence scale associated with viscous dissipation in a building fire. The RANS k–ε turbulence models and LES are both popularly used. However, there are inherent limitations in RANS for modelling transient unsteady flow. The nature of RANS models, however, is a steady-state methodology. Johnson and Hunter [25] showed that the transient flow was a very important factor in modelling passive pollutant concentration fields from wind tunnel experiments. Therefore, RANS models cannot predict accurately the transient wind field and hence is unable to model the turbulent pollutant transport processes under wind condition with good accuracy.

Large Eddy Simulation (LES) is a CFD method capable of predicting unsteadiness and intermittency in turbulent flows. It has been recently widely applied to simulate the turbulent pollutant transport in street canyons and fire-induced flow in fire scenarios. In LES, the large eddy turbulence is directly computed, while the small turbulent motions are modelled by Sub-Grid Models (SGM). Walton et al. [26,27] compared the accuracy of predicted flow in a street canyon by LES and RANS k–ε turbulence closure schemes with field measurements, with results indicated that the LES predictions exhibited the best agreement with the experimental results.

Fire Dynamics Simulator (FDS), which was developed by National Institute of Standards and Technology (NIST), solves numerically a form of the Navier-Stokes equations for thermally driven flow. It is now a popular CFD tool in fire related researches, as well as used to simulate the concentration and flow distribution in urban street canyons [e.g., 10]. In FDS, all spatial derivatives are approximated by second order finite differences and the flow variables are updated in time using an explicit second order predictor-corrector scheme. A description of the model, many validation examples, and a bibliography of related papers and reports may be found on the web at http://fire.nist.gov/fds/. It includes both DNS model and LES model. The FDS LES model is widely used in study of fire-induced smoke transportation and dispersion. FDS solves the basic conservation of mass, momentum and energy equations for a thermally expandable, multi-component mixture of ideal gases. The governing equations are [16]:Conservation of mass:

$$\frac{\partial \rho}{\partial t} + \nabla \cdot \rho u = 0 \tag{1}$$

Conservation of species:

$$\frac{\partial}{\partial t}(\rho Y_l) + \nabla \cdot \rho Y_l u = \nabla \cdot \rho D_l \nabla Y_l + \dot{m}_l''' \tag{2}$$

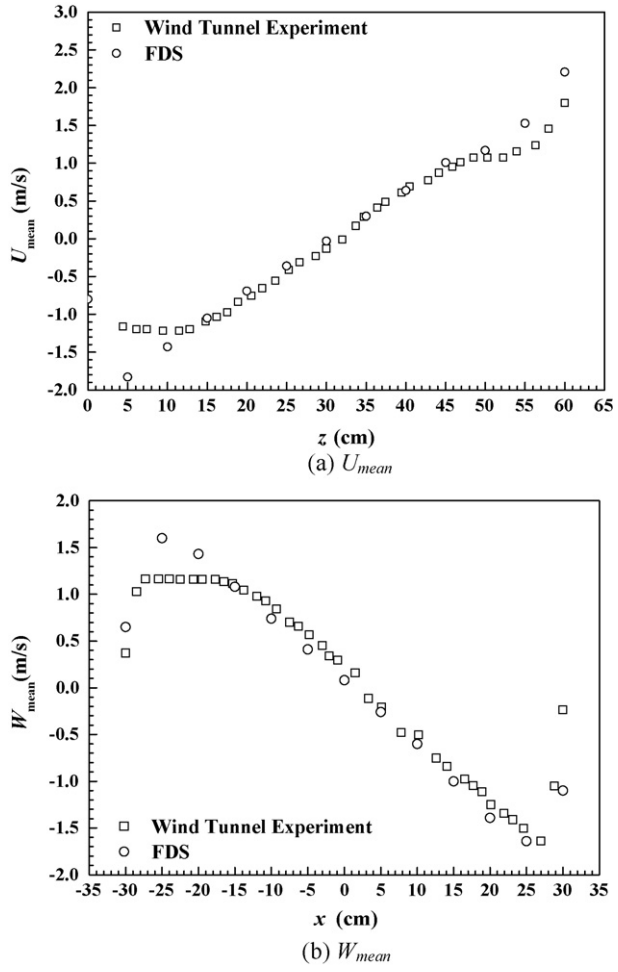

Fig. 2. Comparison of FDS predictions of flow velocity field in the street canyon with wind tunnel experimental data.

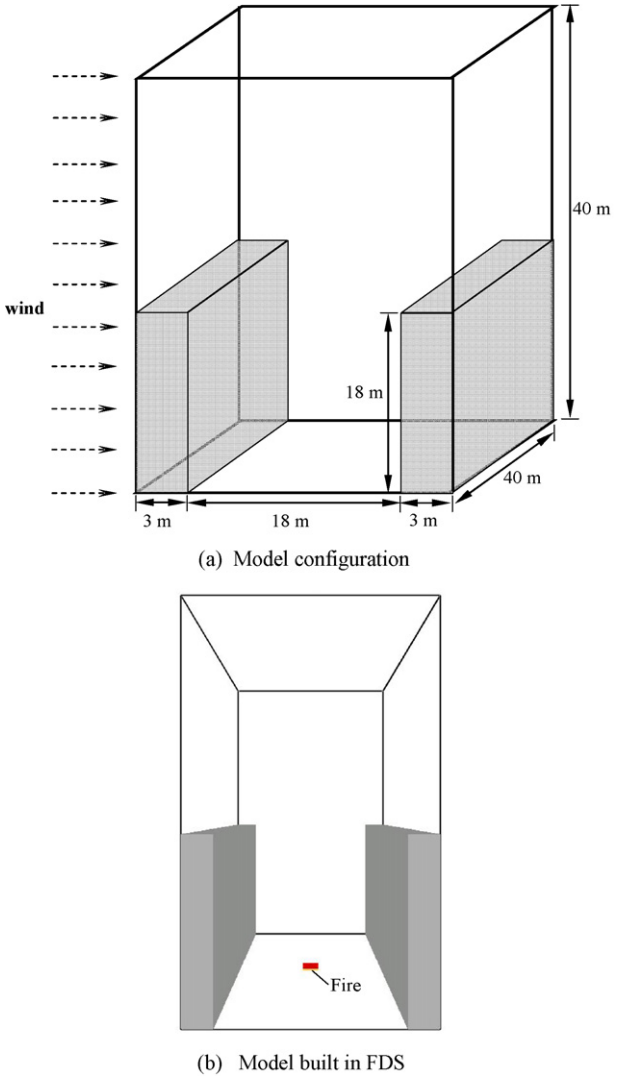

Fig. 3. Model built for LES simulation in FDS.

Conservation of momentum:

$$\rho\left(\frac{\partial u}{\partial t}+(u\cdot\nabla)u\right)+\nabla p=\rho g+f+\nabla\cdot\tau \tag{3}$$

Conservation of energy:

$$\frac{\partial}{\partial t}(\rho h)+\nabla\cdot\rho hu=\frac{Dp}{Dt}-\nabla\cdot q_r+\nabla\cdot k\nabla T+\sum_L\nabla\cdot h_l\rho D_l\nabla Y_l \tag{4}$$

For the numerical solution of the momentum equation, the following is applied by integrating the equation around a closed loop that moves with the fluid, in the absence of any external forces, to identify the sources of vorticity, as well as in the boundary and shear layers [16]:

$$\frac{d\Gamma}{dt}=\oint\frac{1}{\rho_\infty}\left(1-\frac{\rho_\infty}{\rho}\right)\nabla\tilde{p}\cdot dx+\oint\frac{\rho-\rho_\infty}{\rho}g\cdot dx+\oint(\nabla\cdot\tau_{ij})\cdot dx \tag{5}$$

The first term on the right hand side represents the baroclinic torque. The second term is buoyancy-induced vorticity. The third term represents the vorticity generated by viscosity or sub-grid scale mixing, as in boundary and shear layers.

The SGM commonly used in LES was developed originally by Smagorinsky [28]. The eddy viscosity was obtained by assuming that the small scales are in equilibrium, by balancing the energy production and dissipation [29]. A refined filtered dynamics SGM was applied in the FDS LES model to account for the sub-grid scale motion of viscosity, thermal conductivity and material diffusivity [16]. The turbulent viscosity defined in FDS is [16]

$$\mu_{\mathrm{LES}}=\rho(C_S\Delta)^2|S|^{1/2} \tag{6}$$

where C_S is an empirical Smagorinsky constant, Δ is $(\delta x\delta y\delta z)^{1/3}$ and

$$|S|=2\left(\frac{\partial u}{\partial x}\right)^2+2\left(\frac{\partial v}{\partial y}\right)^2+2\left(\frac{\partial w}{\partial z}\right)^2+\left(\frac{\partial u}{\partial x}+\frac{\partial v}{\partial y}\right)^2+\left(\frac{\partial u}{\partial z}+\frac{\partial w}{\partial x}\right)^2+\left(\frac{\partial v}{\partial z}+\frac{\partial w}{\partial y}\right)^2-\frac{2}{3}(\nabla\cdot\vec{u})^2 \tag{7}$$

The term |S| consists of second order spatial differences averaged at the grid center. The thermal conductivity k_{LES} and material diffusivity D_{LES} of the fluid are related to the viscosity μ_{LES} in terms of the Prandtl number Pr and Schmidt number Sc by

$$k_{\mathrm{LES}}=\frac{c_p\mu_{\mathrm{LES}}}{Pr};\quad(\rho D)_{\mathrm{LES}}=\frac{\mu_{\mathrm{LES}}}{Sc} \tag{8}$$

Both Pr and Sc are assumed to be constant. The specific heat c_p is taken to be that of the dominant species of the mixture [16].

The Smagorinsky constant C_S in LES simulation is flow dependent and has been optimized over a range from 0.1 to 0.25 for various flow fields. Zhang et al. [20] had studied the predicted

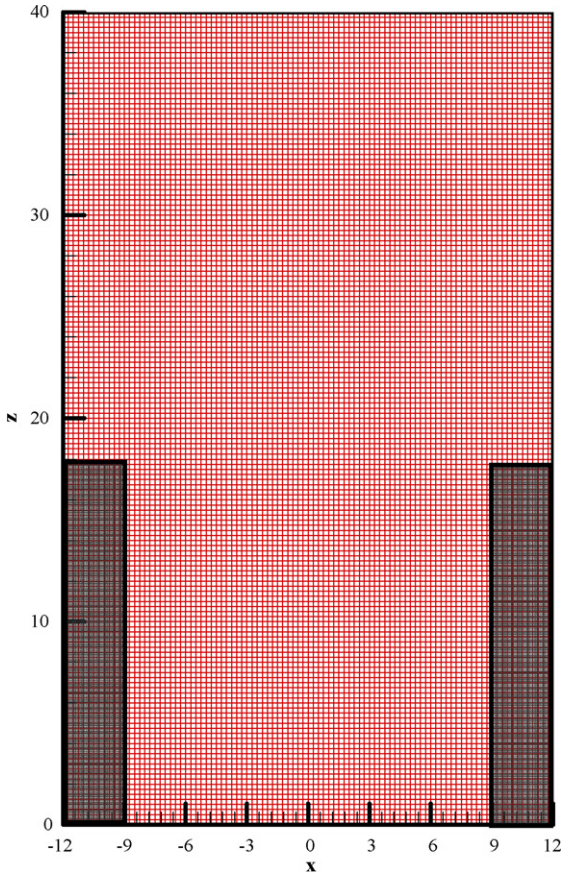

Fig. 4. Grids built for LES simulation in FDS.

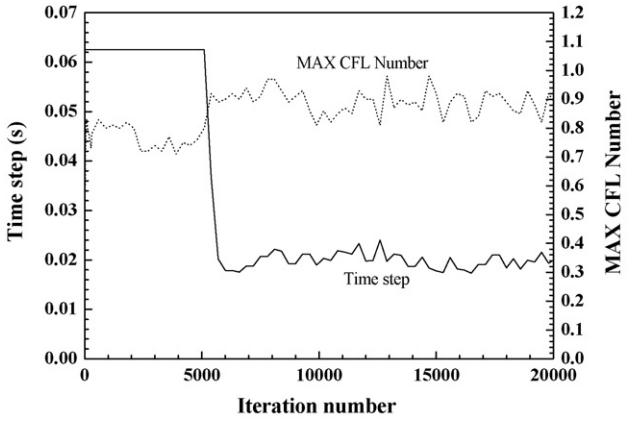

Fig. 5. Time steps and computational convergence for the FDS simulation.

turbulence statistical quantities in a fire room with two values of C_s, 0.14 and 0.18, and two values of P_r, 0.2 and 0.9. Results showed that the predictions are similar under the two different C_s numbers for the weak buoyant plumes. However, for a strong buoyant plume, the predictions of the mean velocity and temperature and also the turbulent statistical quantities using C_s of 0.18 are much better than C_s of 0.14. Comparisons also indicated that setting the P_r to be 0.2 should be more reasonable for simulating the fire. It was also reported [22] that taking C_S as 0.2 gave good predictions for buoyancy-driven flow. FDS had been subjected to many verification works [e.g., 20,30,31] and improved since its first release by NIST in 2000. According to these validation works, the constants C_S, Pr and Sc are set defaulted in FDS for the simulations of this paper as 0.2, 0.2 and 0.5, respectively. It was reported [22] that for simulating buoyancy-drive flow, the predicted values from the filtered dynamics SGM by FDS agreed better with the measured value than those from the original Smagorinsky model and RANS.

For the wall function and the treatment of the vicinity, a tangential velocity boundary condition is used in FDS to control how the gas "sticks" to a solid surface. Ideally, the tangential component of velocity is zero at the surface, but increases rapidly through a narrow boundary layer region, which is typically a few millimeters thick. It is not yet practical to set a fine enough grid to resolve the boundary layer in most practical problems. For this reason, in the FDS LES calculation, the velocity at the wall is set to be a fraction, controlled by a parameter of VBS [16] ranged from −1 to 1, of its value in the grid cell adjacent to the wall. If a no-slip wall is desired, VBC = −1. If a free-slip wall is desired, VBC = 1. Numbers in between −1 and 1 can represent partial slip conditions, which may be appropriate for simulations involving large grid cells. The Default VBC is 0.5 for LES in FDS, which implies that the velocity at the wall is approximated to be half of that in the grid cell adjacent to the wall.

The initial time step is set automatically in FDS by the size of a grid cell divided by the characteristic velocity of the flow. The default value of the initial time step is $5(\delta x\delta y\delta z)^{1/3}/\sqrt{gH}$, where δx, δy, and δz are the dimensions of the smallest grid cell, H is the height of the computational domain, and g is the acceleration due to gravity [16]. The Courant-Friedrichs-Lewy (CFL) criterion [20,29] is used along with the above setting of the time step in FDS [16] for justifying the computational convergence. This criterion is more important for large-scale calculations where convective transport dominates the diffusive one. In FDS, the estimated velocities are tested at each time step to ensure that the following CFL criterion is satisfied [16]:

$$\delta t \cdot \max\left(\frac{|u_{ijk}|}{\delta x}, \frac{|v_{ijk}|}{\delta y}, \frac{|w_{ijk}|}{\delta z}\right) < 1 \tag{9}$$

During the calculation, the time step is varying and constrained by the convective and diffusive transport speeds to ensure that the CFL condition is satisfied at each time step [16]. The time step will eventually get to be a quasi-steady value when the flow field reaches a quasi-steady state.

2.2. Model validation

In order to validate FDS in simulating the flow profile in the street canyon, since FDS cannot offer the function of setting up the value of the inlet turbulence intensity, the wind tunnel experiments by P. Salizzoni et al. [32] was further used to compare with FDS predictions with a uniform inlet wind flow boundary condition. The street canyon model in the wind tunnel experiment was 0.06 m wide and 0.06 m high, with a horizontal constant external wind flow of 6.8 m/s. The comparison of experimental data and FDS predictions, for the profiles of the mean horizontal velocity U, as a function of height z at the mid-length of the canyon, and of the mean vertical velocity W, as a function of x, at the canyon mid-height, are shown in Fig. 2. It was shown that FDS well predicts the experimental values.

The FDS code had also been validated to be capable of modelling gas dispersion under wind flow in a tunnel as well as in a street canyon. For example, the predicted CO dispersion in a fire by FDS was proved by Hu et al. [18], to be in good agreement with the full scale measured data in an 88 m long channel. Chang et al. [10] also compared the concentration and flow distribution in urban street canyons predicted by FDS LES model and FLUENT RANS k–ε model

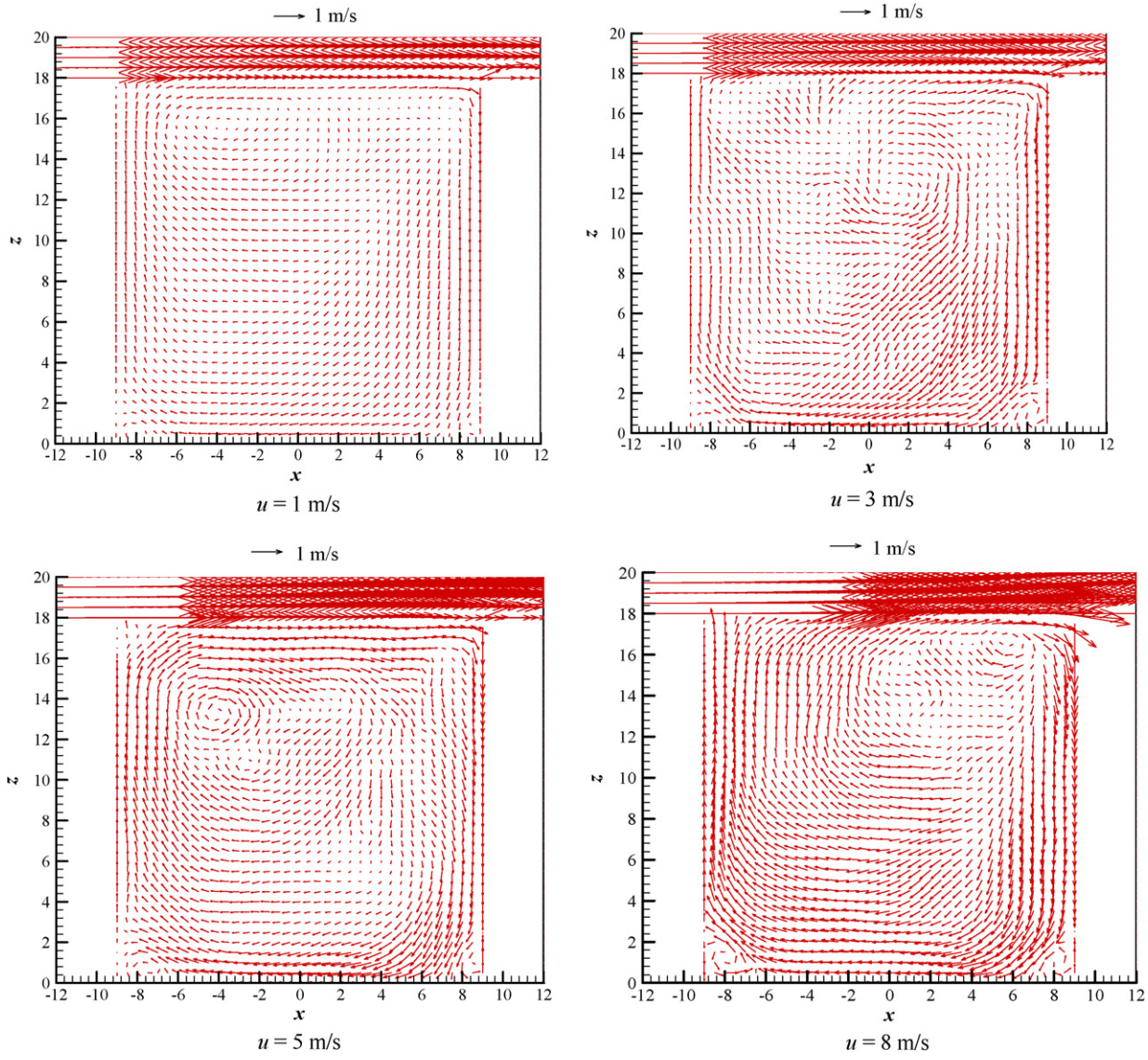

Fig. 6. Velocity vector field predicted by FDS with no fire in the street canyon.

with wind tunnel experiments. The results from the FDS LES were reported to agree much better with the experimental results than those from FLUENT RANS k–ε model. However, another important feature of the simulation study in this paper, that should be considered, is the turbulence due to the interaction between the plume buoyancy and the wind flow inertial force. Validation work of FDS LES predictions for the development of large fire plume under the force of horizontal cross wind flow had also been formerly conducted by Hu et al. [33,34]. The predicted plume temperature was compared with full scale measured data in a real road tunnel under a longitudinal cross wind flow. It was shown that the plume temperatures predicted by FDS LES were in good agreement with full scale experimental data.

2.3. Model configuration

A domain of 24 m wide, 40 m long and 40 m high was built for CFD simulation as shown in Fig. 3(a). Two buildings of 3 m wide, 40 m long and 18 m high, the same as that used by Baker et al. [4], were set at both sides of the domain to create an idealized street canyon of 18 m wide and 18 m high with an aspect ratio (W/H) of 1, which was the same as the one used by Baker et al. [4]. The 3-D simulation domain built by FDS was shown in Fig. 3(b).

An inlet velocity boundary condition was set at the left side of the simulation domain. The top and the other three sides of the domain were all set to be naturally opened [16] with no initial velocity boundary condition specified for these openings. There were two kinds of settings of the inlet velocity boundary positions reported in the literatures: setting the inlet velocity boundary of the computational domain away from, or horizontally directly levelling to, the windward face of the first building. The flow field in the street canyon differs with different distances of the inlet velocity boundary to the windward face of the first building in the first kind of setting method. In order to purely investigate the interaction between the buoyancy driven flow and the initial circulation flow in the street canyon, the second kind of setting method, which was mainly used [e.g., 4,6,26,27] in considering the pollutant dispersion in the street canyon under different levels of perpendicular wind flows, was selected. The inlet flow turbulence should be considered carefully for such a CFD calculation. In former literatures [e.g., 4,6,26,27], the turbulence fluctuation of the inlet flow was specified by periodic (or cyclic) inlet–outlet boundary conditions. But FDS does not offer the function of setting up the value

of the inlet turbulence intensity. However, it was validated above, as well as reported in literature [10], that for street canyon with $W/H = 1$, the FDS still predicted the measurements of flow velocity field in the wind tunnel experiments in good agreement with a uniform inflow boundary condition with no turbulence intensity specified. It was also concluded [32] that the turbulence level inside the canyon is not very sensitive to the external turbulence condition for s square canyon in the skimming flow regime, since the shear layer at the interface acts as a filter for the incoming turbulent structures. So, a uniform cross wind flow was set to blow into the domain from the left side. The Reynolds number of the inlet flow, defined by $Re = uH/\nu$ where ν is the dynamic viscosity of air, in the range of about $0.6–6 \times 10^6$ with wind velocity of 0.5–5 m/s.

Square pool fires were set as buoyancy source at the centre of the street canyon to produce buoyancy driven plume flow. The buoyancy release rate of a fire is generally quantified by its Heat Release Rate (HRR), Q. The HRR was set in FDS by the fire source area along with the parameter "Heat Release Rate Per Unit Area (command "HRRPUA" provided in FDS)". The HRRs considered for fire sources in the simulations were 0.5 MW (0.5 m^2), 1 MW (1.0 m^2), 3 MW (3.0 m^2), 5 MW (5.0 m^2), 8 MW (8.0 m^2), 10 MW (10.0 m^2), 15 MW (15.0 m^2) and up to 20 MW (20.0 m^2) with a steady HRRPUA of 1000 kW/m^2. However, a burning car or bus typically produces a fire with HRR of 5 MW and 20 MW, respectively [35,36].

In LES simulation, the grid size is also an important factor to be considered as well as the SGM. It should be fine enough to include the turbulence scales associated with the largest eddy motions which can be described accurate enough by the SGM. Balance should be considered for the gird size and the computation effort. Smaller gird size gives detailed information of the flow but needs more computation resource and longer computing time. However, the basis of large eddy simulation is that accuracy increases as the numerical mesh is refined. In a former LES study conducted by Baker et al. [4] for a street canyon with same configuration as the one in this paper, the grid size in the x- and y-direction was set to be 0.3 m and 1.0 m, respectively. In the z-direction, the grid size was set to be 0.3 m in the street canyon and increased to be a maximum dimension of 5 m above the roof level of the canyon. For the simulation of this paper, a smaller uniform gird system was used. The gird number was $96 \times 160 \times 160$ in the x- , y- and z-direction, respectively (total 2,457,600 grids) with uniform gird size of 0.25 m as shown in Fig. 4.

For all the cases with wind flow, the simulations were run for a primary time period of 300 s to generate the original air flow field in the street canyon. Then, the fire was started as the buoyancy source to produce the buoyant plume flow. So, the interaction between the buoyancy driven plume flow and the original wind flow was simulated. All the simulations were run for a total simulation time of 1200s when the flow field was shown to be already quasi-steady, in a personal computer with new generation of 64 bit CPU of Intel Core 2 Duo E6300 (1.86 G Hz) and memory size of 2 G. The CFL numbers and the time steps during one simulation are typically shown in Fig. 5. The time step in the initial 300 s without buoyant fire source was maintained at 0.0625s when the flow field was steady. When the buoyant fire source started after 300 s, the time step decreased to be oscillating quasi-steady values averaged at 0.02 s. The CFL numbers during the iterations were in the range of 0.12–0.98, all less than the criteria value of 1. The CFL convergence criterion was satisfied.

3. Results and discussion

The velocity vector field predicted by FDS with no buoyancy source, under different perpendicular wind flow velocities, in the street canyon is shown in Fig. 6. It can be seen that a large recirculation flow was mainly formed with still some small vortexes, in the street canyon. The main recirculation flow came down into the street canyon along the wall of the leeward building until to the base level, flowed along the base ground of the street canyon in the windward direction, turned upward along the wall of the windward building, then suppressed by the perpendicular wind to flow in the horizontal downstream direction when reached the top of the street canyon and was re-entrained back into the street canyon again. This was in accordance with former researches [e.g., 1,4,6] on the flow pattern in the street canyon under this condition. It was also shown that with the increase of the wind flow velocity, the recirculation flow velocity also increased.

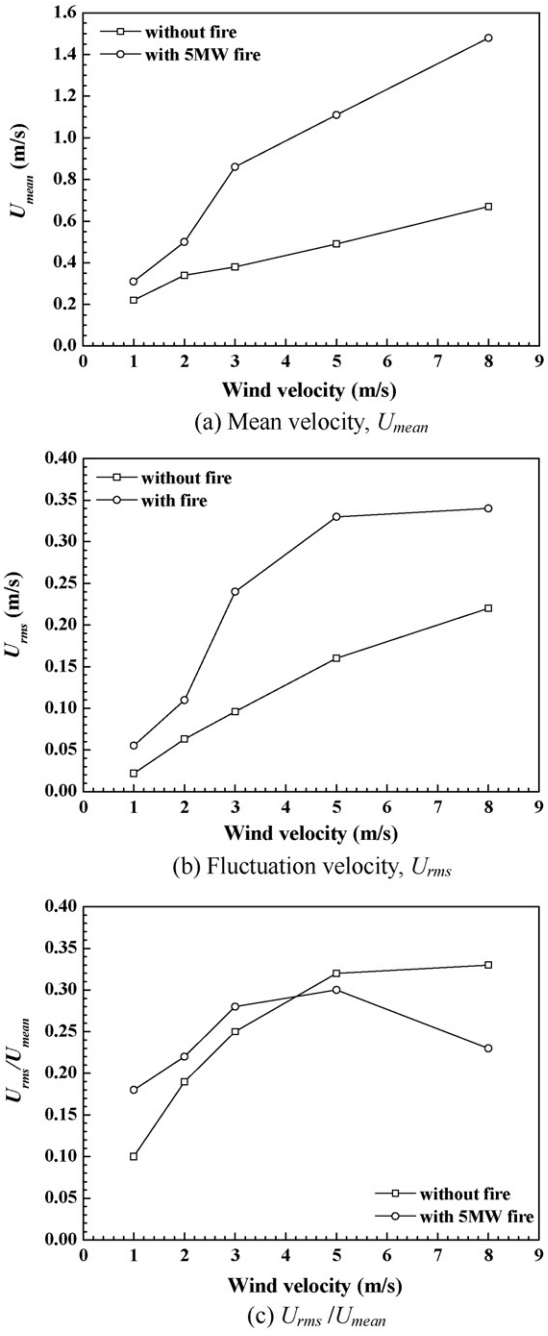

Fig. 7. Flow turbulence statistics near the floor under different levels of perpendicular wind flow.

Fig. 7 presents the flow turbulence statistics in the horizontal direction, U, near the canyon floor (at 0.5 m above the floor and

1 m away from the right side of the fire source) under different levels of perpendicular wind flow. It was shown that both the mean flow velocity and the flow turbulence fluctuation velocity increased with the increase of the wind flow velocity. When there is a buoyant fire source in the street canyon, both the mean flow velocity and the flow turbulence fluctuation velocity also increased remarkably. This indicated that the entrainment of the buoyant fire source and the plume enhanced the horizontal mean flow velocity near the floor as well as its turbulence. However, the relative ratio of the fluctuation velocity to the mean velocity seemed to first increase before the wind flow velocity reached 5m/s. After that, the value of U_{rms}/U_{mean} seemed to change small without fire, and even some decrease with a 5 MW fire, with the increase of the wind flow velocity.

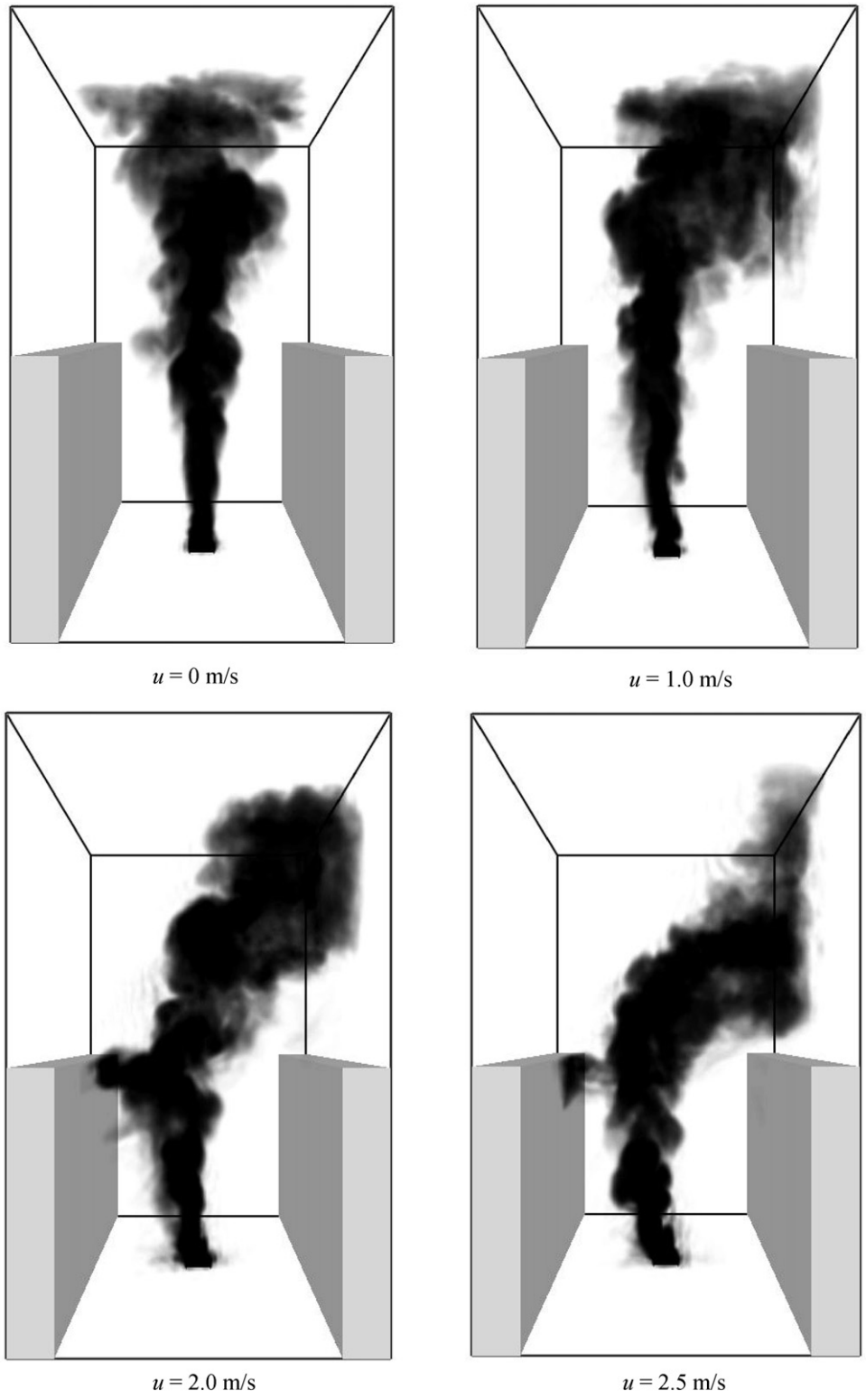

Fig. 8. Buoyant smoke plume dispersion in and above the street canyon under different levels of perpendicular wind flow.

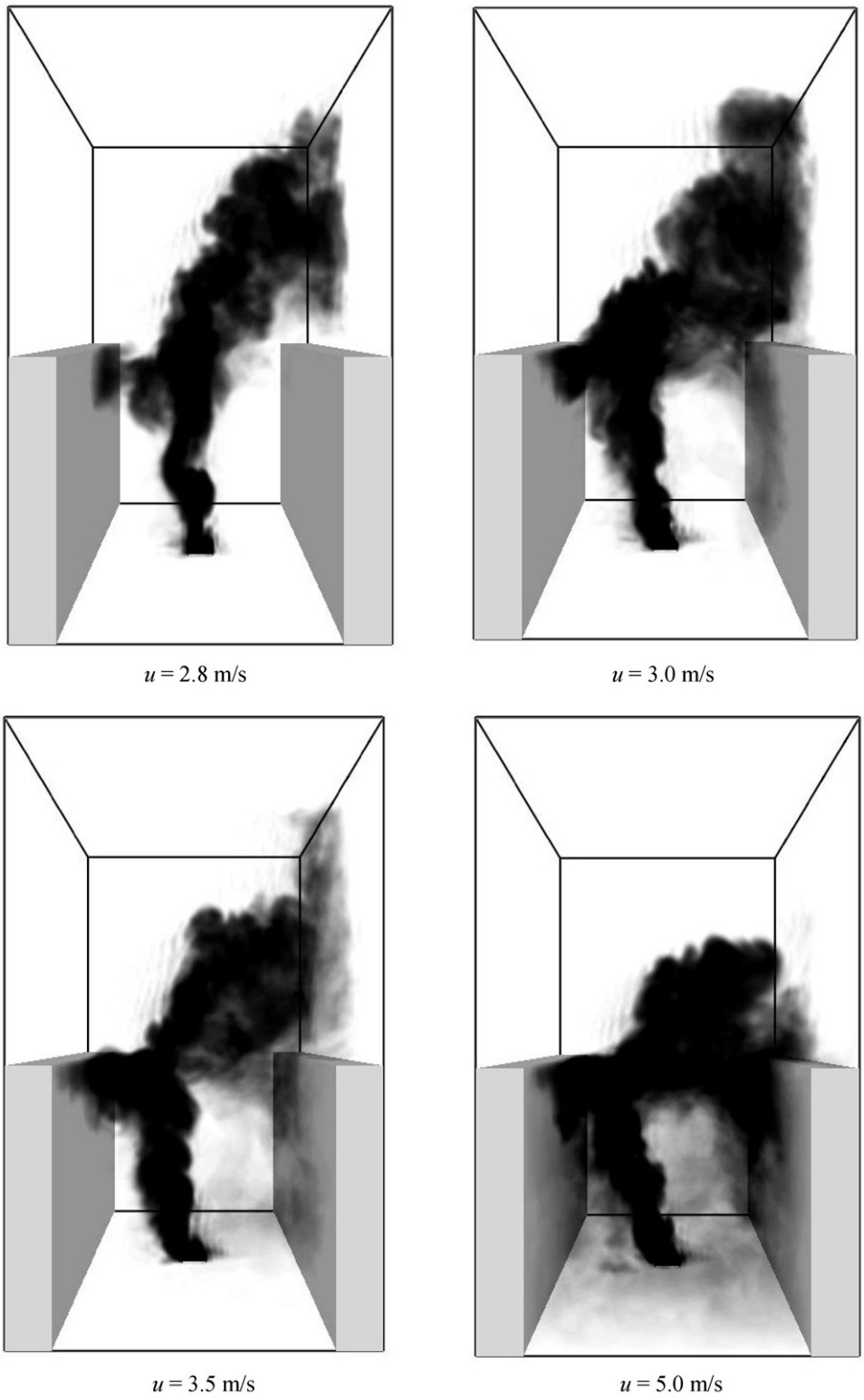

Fig. 8. (*Continued*)

$u = 8.0$ m/s

Fig. 8. (*Continued*).

The buoyancy driven plume dispersion (soot density field) in and above the street canyon under different levels of perpendicular wind flow, when the flow field is already quasi-steady, is shown in Fig. 8. It can be seen that with the increase of the wind flow velocity, the plume dispersion pattern fell into four regimes:

- Regime I, with zero or very small wind velocity (for example, 1 m/s in this case). With zero wind velocity, the fire plume rose up straight vertically, entraining fresh air from around and the radius of the plume grew up axis-symmetrically. Under the wind condition with very lower velocity, the buoyant plume just tilled a little under the "push" force of the wind flow. However, the plume did not tough the walls of the buildings at both sides of the street canyon. All the smoke was ventilated out of the top of the street canyon freely by the aid of its own buoyancy.
- Regime II, with light wind velocity (for example, 2.0 m/s, 2.5 m/s and 2.8 m/s in this case). In this regime, with the increase of the perpendicular wind flow velocity, some of the smoke accumulated in the windward part of the street canyon and touched the windward building, just like a "nose" grew out from the plume and was cut to be flat by the wind flow at the top of the windward building. The accumulated harmful smoke will be dangerous for the people in the compartments at the top part of the windward building if there are openings to the street canyon. However, the plume did not touch the wall of the building at the leeward direction.
- Regime III, with breeze or moderate wind flow (for example, 3 m/s, 3.5 m/s and 5 m/s in this case). In this regime, the buoyant plume in the street canyon tilled to the windward direction significantly and finally directly impinged onto the wall of the windward building. With the increase of the wind velocity, the horizontal length of the "nose" increased. Another important characteristic for this regime was that part of the pollutant plume smoke was re-entrained back into the street canyon along the wall of the leeward building and filled the entire street canyon. This is a serious situation as the re-entrained smoke will be harmful and toxic for the people in the street canyon as well as that in the building with openings to the street canyon. The wind velocity under which the buoyancy driven rising pollutant plume was re-entrained back into the street canyon along the wall of the leeward building was defined as "critical re-entrainment wind velocity" here.
- Regime IV, with strong wind flow (for example, 8 m/s in this case). In this regime, almost all the smoke plume rising up was re-entrained back into the street canyon with little of them escaped from the top of the street canyon in the leeward direction. The smoke will mostly accumulate in the street canyon with little naturally being ventilated by its own buoyancy force. And the fire plume in the street canyon tilled largely under this condition and finally even directly attached to the wall of windward building. The windward building surface (including the wall and the window) will be directly heated and even damaged by the hot fire plume.

The smoke temperature contours in and above the street canyon under different levels of perpendicular wind flow is also shown in Fig. 9. The four dispersion pattern regimes of the fire plume can also be clearly identified. So, it was shown that the pollutant dispersion induced by a buoyancy source should be quite different from that without buoyancy. In the case of with no buoyancy, it is known that the strong wind helps the air circulation in the street canyon. More pollutant will be taken out of the top of the street canyon with stronger wind flow. However, this is not the case with a buoyancy source in the street canyon. The pollutant can initially escape vertically from the top of the street canyon by the aid of its own buoyancy. But the wind flow trends to form a circulation flow in the street canyon, which counteracts the buoyancy driven flow and will take the buoyant pollutant that rises up to the top of the canyon back to the street ground level. When the wind velocity increased to a certain level, the hot gases of the fire plume was re-entrained back into the street canyon and mixed with the original ambient air in the street canyon. However, it should be also noted in Fig. 9 that the temperature of the smoke that was re-entrained back into the street canyon is only about 1–2 $^\circ$ above the ambient, indicating

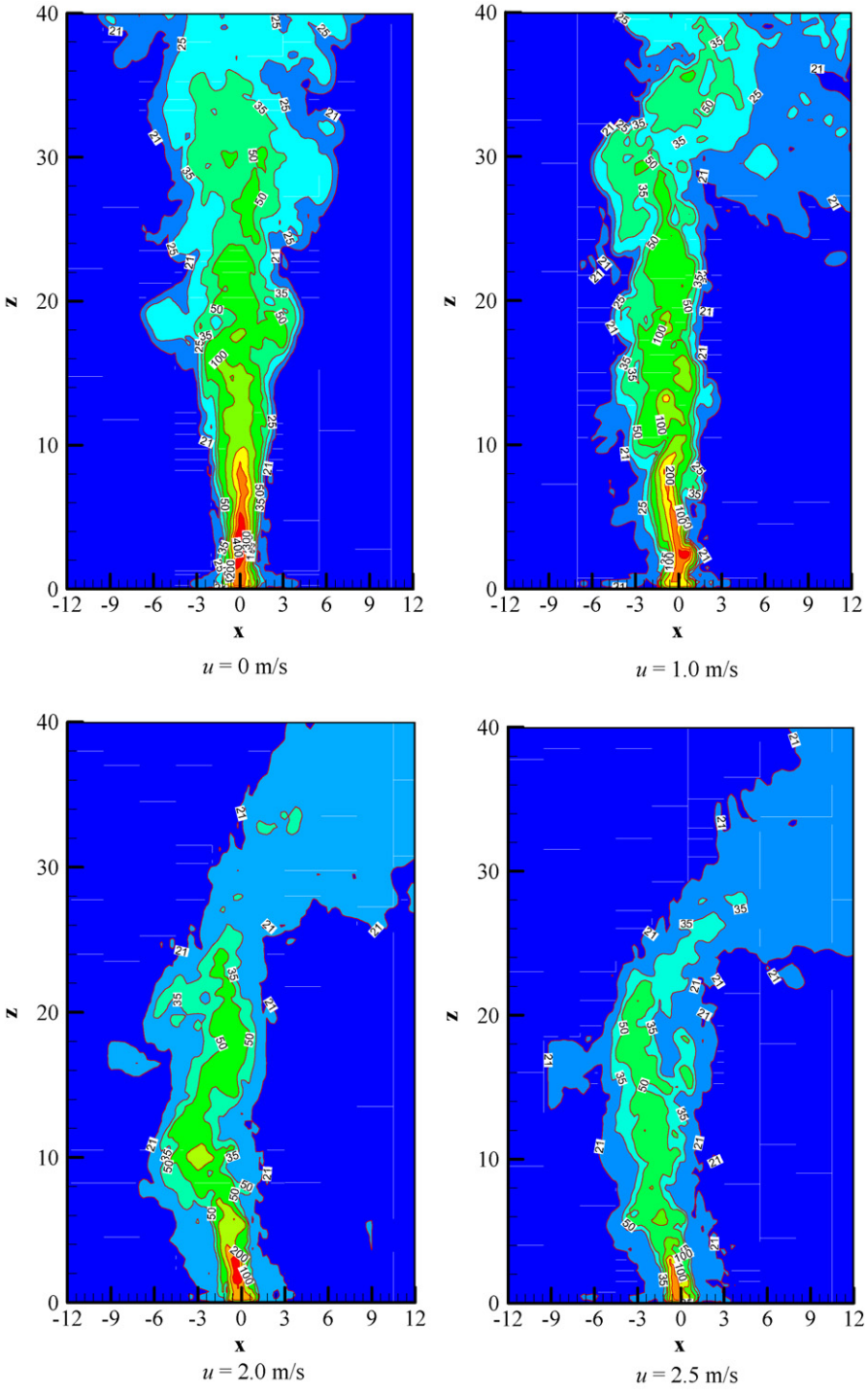

Fig. 9. Smoke temperature contours in and above the street canyon under different levels of perpendicular wind flow.

its buoyancy is very too small to drive them to be ventilated out. But at the same time, the smoke density was seemed to be dense in the street canyon referring Fig. 8. From above, it can be drawn that the fire occurred in a street canyon produces large amount of harmful smoke, which should be much denser than that emitted by the engines of running vehicles. The smoke plume can initially be ventilated out of the street canyon by its own strong buoyancy. But it should be do concerned that it is possibly to be re-entrained back into the street canyon with little buoyancy left due to the effect of a perpendicular wind flow, being hardly to be ventilated out by its own buoyancy any more then and finally accumulated within the street canyon to high levels to threat the human safety.

So, it can be seen that the critical wind velocity under which the pollutant buoyant plume smoke was re-entrained back into the street canyon is a very important parameter to be concerned. This critical re-entrainment wind velocity should relate to the HRR of the fire buoyancy source, and also the height and width of the street canyon. For the street canyon of this paper, the critical re-entrainment wind velocity is plotted against the HRR of the fire in Fig. 10. It can be seen that the critical re-entrainment wind velocity

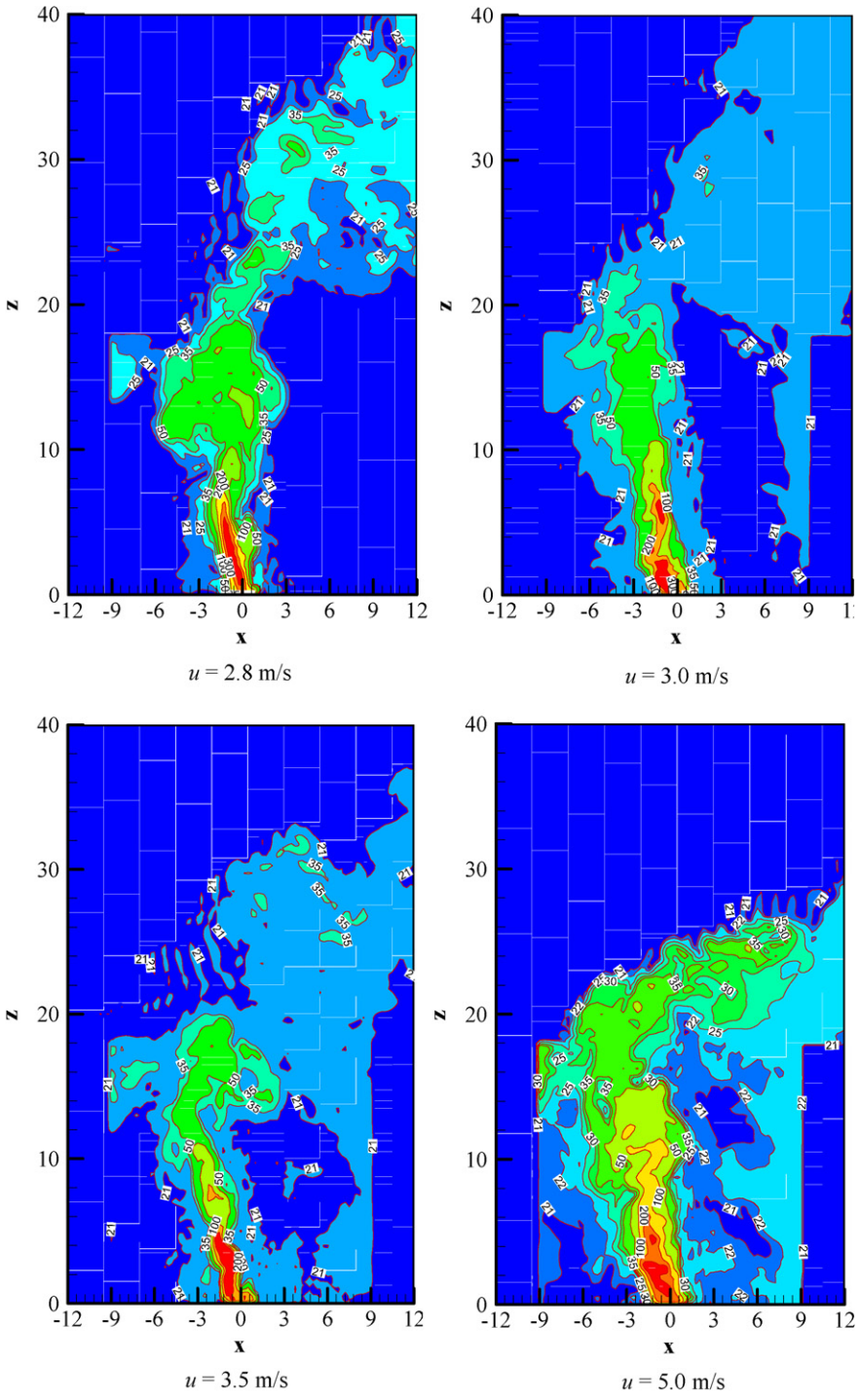

Fig. 9. (*Continued*)

increased asymptotically with the HRR of the fire. The critical re-entrainment wind velocity increased more significantly with the HRR at smaller fires than that at larger fires. And finally, the critical re-entrainment wind velocity seemed to change little with the increase of the HRR of the fire any more. However, for the case of burning a car or a bus in such a street canyon, corresponding to the HRR of about 5 MW or 20 MW, the critical re-entrainment wind velocity was 3.0 m/s and 3.9 m/s, respectively. According to the wind power grades defined in meteorology, such two wind speeds are just classified in level 2 and level 3 as light wind and breeze wind, respectively. These levels of wind speed are very usual in urban areas. So, it can be seen that this re-entrainment phenomenon of fire plume is very easy to occur in case of a car or a bus accidentally burning in such a street canyon. It is a significant situation that we should pay attention to, concerning the safety of people in the street canyon.

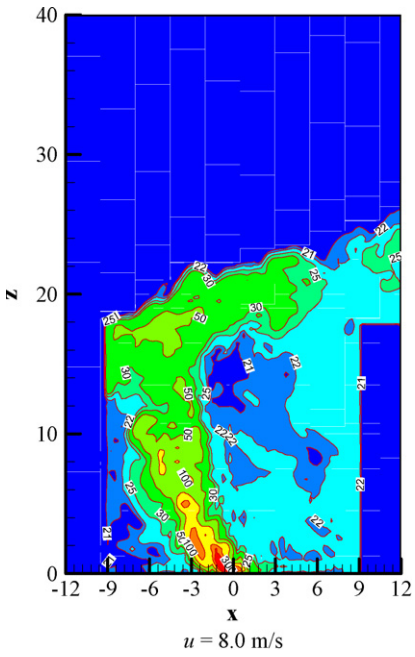

Fig. 9. (*Continued*).

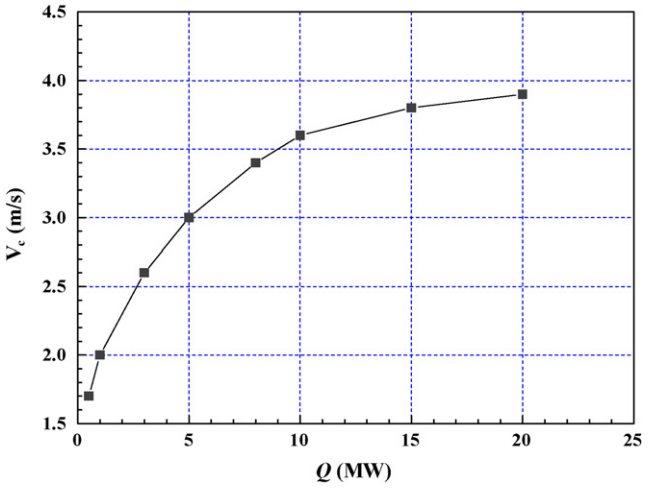

Fig. 10. Critical re-entrainment wind velocity (V_c) vs. heat release rate of the fire (Q).

4. Conclusions

LES simulation was performed in this paper to study the dispersion of fire-induced buoyancy driven smoke plume in and above an urban street canyon with perpendicular wind flow to its axis, as a result that should be concerned of the complicated interaction between the buoyancy force of the fire plume and the inertial force of the coming wind flow in such an urban component.

It was revealed that, as the velocity of the wind flow that coming across the top of the street canyon increasing from 0 m/s to be higher, the dispersion pattern of the fire plume under this condition fell into four regimes. There was a critical re-entrainment wind velocity that when the wind flow velocity increased to this level, the primary uprising buoyant fire plume escaping from the top of the street canyon due to its own buoyancy would be re-entrained back into the street canyon. The street canyon would be filled and polluted by the harmful fire smoke under this condition, threatening the safety of the people in the street canyon. This re-entrainment phenomenon seemed to be easy to occur when a car or a bus accidentally burning in such a street canyon, as the critical re-entrainment wind velocity under this condition just fell into a level 2 (light wind) or level 3 (breeze wind) wind power grade, being very usual in urban areas.

The variation of the critical re-entrainment wind velocity along with the increase of the HRR of the fire was further studied to show that the critical re-entrainment wind velocity increased asymptotically with the HRR of the fire. However, other factors influence the critical re-entrainment wind velocity should include the configuration, such as width and height, of the street canyon. The effects of the turbulence intensity and length scale of the flow in and above the street canyon also need to be quantified. These will be further investigated. A more detailed and systematic experimental study will also be carried out in a wind tunnel and reported in the future.

Acknowledgements

This work was supported by Natural Science Foundation of China under Grant No. 50706050.

References

[1] T.R. Oke, Street design and urban canopy layer climate, Energy Build. 11 (1988) 103–113.
[2] Y.A. Gayev, E. Savory, Influence of street obstructions on flow processes within street canyons, J. Wind Eng. Ind. Aerodyn. 82 (1999) 89–103.
[3] S. Xie, Y. Zhang, L. Qi, X. Tang, Spatial distribution of traffic-related pollutant concentrations in street canyons, Atmos. Environ. 37 (2003) 3213–3224.
[4] J. Baker, H.L. Walker, X.M. Cai, A study of the dispersion and transport of reactive pollutants in and above street canyons—a large eddy simulation, Atmos. Environ. 38 (2004) 6883–6892.
[5] S.-K. Park, S-D. Kim, H. Lee, Dispersion characteristics of vehicle emission in an urban street canyon, Sci. Total Environ. 323 (2004) 263–271.
[6] J.-J. Baik, Y.-S. Kang, J.-J. Kim, Modeling reactive pollutant dispersion in an urban street canyon, Atmos. Environ. 41 (2007) 934–949.
[7] L.X. Li, J.S. Wang, X.D. Tu, W. Liu, Z. Huang, Vertical variations of particle number concentration and size distribution in a street canyon in Shanghai, China, Sci. Total Environ. 378 (2007) 306–316.
[8] M. Pavageau, M. Schatzmann, Wind tunnel measurements of concentration fluctuations in an urban street canyon, Atmos. Environ. 33 (1999) 3961–3971.
[9] P. Kastner-Klein, E. Fedorovich, M.W. Rotach, A wind tunnel study of organised and turbulent air motions in urban street canyons, J. Wind Eng. Ind. Aerodyn. 89 (2001) 849–861.

[10] C.-H. Chang, Computational fluid dynamics simulation of concentration distributions from a point source in the urban street canyons, ASCE-J. Aerospace Eng. 19 (2) (2006) 80–86.
[11] X.-X. Li, C.-H. Liu, D.Y.C. Leung, K.M. Lam, Recent progress in CFD modelling of wind field and pollutant transport in street canyons, Atmos. Environ. 40 (2006) 5640–5658.
[12] J. Ovadnevaite, K. Kvietkus, A. Marsalka, Summer fires in Lithuania: impact on the Vilnius city air quality and the inhabitants health, Sci. Total Environ. 356 (2006) (2002) 11–21.
[13] Y. Alarie, Toxicity of fire smoke, Critical Rev. Toxicol. 32 (2002) 259–289.
[14] R. Besserre, P. Delort, Recent studies prove that the main cause of death during urban fires is poisoning by smoke, Urgences Medicales 16 (1997) 77–80.
[15] K. McGrattan, G. Forney, Fire Dynamics Simulator (Version 4.07) User's Guide, National Institute of Standards and Technology, 2006.
[16] K. McGrattan, Fire Dynamics Simulator (Version 4.07) Technical Reference Guide, National Institute of Standards and Technology, 2006.
[17] L.H. Hu, W. Peng, R. Huo, Critical wind velocity for arresting upwind gas and smoke dispersion induced by near wall fire in a road tunnel, J. Hazard. Mater. 150 (2008) 68–75.
[18] L.H. Hu, N.K. Fong, L.Z. Yang, W.K. Chow, Y.Z. Li, R. Huo, Modeling fire-induced smoke spread and carbon monoxide transportation in a long channel: Fire Dynamics Simulator comparisons with measured data, J. Hazard. Mater. 140 (2007) 293–298.
[19] A. Murata, S. Mochizuki, Large eddy simulation of turbulent heat transfer in an orthogonally rotating square duct with angled rib turbulators, J. Heat Transfer (Trans. ASME) 123 (2001) 858–867.
[20] W. Zhang, A. Hamer, M. Klassen, D. Carpenter, R. Roby, Turbulence statistics in a fire room model by large eddy simulation, Fire Safety J. 37 (2002) 721–752.
[21] L.D. Dailey, N. Meng, R.H. Pletcher, Large eddy simulation of constant heat flux turbulent channel flow with property variations: quasi-developed model and mean flow results, J. Heat Transfer (Trans. ASME) 125 (2003) 27–38.
[22] Y. Jiang, Q.Y. Chen, Buoyancy-driven single-sided natural ventilation in building with large openings, Int. J. Heat Mass Transfer 46 (2003) 973–988.
[23] P.J. Mason, N.S. Callen, On the magnitude of the subgrid-scale eddy coefficient in large-eddy simulations of turbulent channel flow, J. Fluid Mech. 162 (1986) 439–462.
[24] M. Germano, U. Piomelli, P. Mion, W.H. Cabot, A dymamic subgrid-scale eddy viscosity model, Phys. Fluids A 3 (1991) 1760–1765.
[25] G.T. Johnson, L.J. Hunter, Urban wind flows: wind tunnel and numerical simulations—a preliminary comparison, Environ. Model. Softw. 13 (1998) 279–286.
[26] A. Walton, A.Y.S. Cheng, W.C. Yeung, Large-eddy simulation of pollution dispersion in an urban street canyon—part I: comparison with field data, Atmos. Environ. 36 (2002) 3601–3613.
[27] A. Walton, A.Y.S. Cheng, Large-eddy simulation of pollution dispersion in an urban street canyon—part II: idealised canyon simulation, Atmos. Environ. 36 (2002) 3615–3627.
[28] J. Smagorinsky, General circulation experiments with primitive equations-I, the basic experiment, Monthly Weather Rev. 91 (1963) 99–105.
[29] P.D. Lax, Hyperbolic difference equations: a review of the courant-friedrichs-lewy paper in light of recent developments, IBM J. Res. Dev. 11 (1967) 235–238.
[30] J.X. Wen, K. Kang, T. Donchev, J.M. Karwatzki, Validation of FDS for the prediction of medium-scale pool fires, Fire Safety J. 42 (2007) 127–138.
[31] P. Friday, F.W. Mowrer, Comparison of FDS Model Predictions with FM/SNL Fire Test Data. NIST GCR 01-810, National Institute of Standards and Technology, Gaithersburg, Maryland, April 2001.
[32] P. Salizzoni, N. Grosjean, P. Mejean, R.J. Perkins, L. Soulhac, R. Vanliefferinge, Wind tunnel study of the exchange between a street canyon and the external flow, Air Pollution Modeling and Its Application XVII, Springer Science+Business Media, LLC, 2007, pp. 430–437.
[33] L.H. Hu, R. Huo, W. Peng, W.K. Chow, R.X. Yang, On the maximum smoke temperature under ceiling in tunnel fires, Tunn. Undergr. Sp. Technol. 21 (2006) 650–655.
[34] L.H. Hu, R. Huo, W.K. Chow, Studies on buoyancy-driven back-layering in tunnel fires, Exp. Therm. Fluid Sci. 32 (2008) 1468–1483, doi:10.1016/j.expthermflusci.2008.03.005.
[35] G.B. Grant, S.F. Jagger, C.J. Lea, Fire in tunnels, Phil. Trans. R. Soc. Lond. A 356 (1998) 2873–2906.
[36] Y.P. Cheng, R. John, Experimental research of motorcar fire, J. China Univ. Mining Technol. 31 (2002) 557–560 (in Chinese, with English abstract).